Theoretical Investigation of Linker Effects on New Designed Bodipy-Ferrocene Based Three Channels Calcium (II) Ion Sensors; as Redox, Colorimetric and Fluorescent Properties

Samira Jeddi and Fatma Sevin*

Faculty of Science, Department of Chemistry, Hacettepe University, 06800 Beytepe, Ankara, Turkey

Address for Correspondence
Fatma Sevin, Faculty of Science, Department of Chemistry, Hacettepe University, 06800 Beytepe, Ankara, Turkey, E-mail: sevin@hacettepe.edu.tr

Keywords: Fluorescence; Sensor; Ferrocene; BODIPY; Conjugated fluorophore; Three channel sensor

Abstract

In this work, the structural, spectroscopic and electronic properties of proposed model complexes of 4,4-Difluoro-4-borata-3a-azonia-4a-ana-s-indacene(BODIPY)-Ferrocene based Calcium ion sensors were investigated by means of DFT calculations. Geometric, and electronic effects of 4 different chemical linkers, azin(1), azadiene(2), urea(3) and thiazole(4), were predicted on the development of these fluorescent sensors computationally at B3LYP/LANL2DZ level. Designed sensors are expected to work in living systems, so all the calculations were carried out in water phase. In addition, frontier molecular orbital properties, electronic spectra and electrochemical properties were also computed. According to the computational thermodynamic results, sensors which contain urea and thiazole as the linker group, make the most stable complexes with Ca(II) ion. In general, it was found that calcium complexation of sensors leads to lower absorption energy bands, causes a decrease in HOMO-LUMO gap with respect to the linker type, a bathochromic shift in the lowest energy absorbance wavelengths, and an anodic shift of redox potential. Overall result of complexation is an increase in the absorption λ_{max} value, while solvent effect causes a blue shift in absorption bands. Maximum emission redshift is observed in urea bridged sensors, followed by thiazole. This sequence was also spotted in the acidic environment. Molecular logic gates are also formed for normally protonated sensors and their metal complexes. Each type of designed sensors is corresponded to a certain type of logic gates.

Introduction

Parallel to the continuous shrinking of the optoelectronic devices such as molecular electronics and information delivery systems in the last decade, interests in the molecular devices has increased extremely. The most important feature of these molecular devices is being a molecular switch [1]. The most important feature of the molecular switches is to show reversible optical and electronic properties which vary in response to various environmental stimuli [2]. There is an enormous demand for chemical sensors for many areas and disciplines. High sensitivity and ease of operation are two main issues for sensor development. Fluorescence techniques can easily fulfill these requirements and therefore fluorescent-based sensors appear as one of the most promising candidates of chemical sensing. Day after day, these sensors improved from one-way to multiple channel sensors in order to be unrivaled sensitive (even just a single metal detection at very low concentrations) [3]. A typical fluorescent sensor combines an analyte recognition site with a fluorescent reporter moiety which translates the binding between the analyte and the recognition site into a fluorescent output signal. The design of fluorescent molecular sensors revolves around three basic concepts: the fluorophore, the recognition mechanism and the fluorescence signaling profile. Various fluorophores have been used in the designing of fluorescent sensors of metal cations. BODIPY is a particularly interesting fluorophore, in the field of molecular sensor designing due to its intense absorption of visible light, high fluorescence quantum yield and excellent photostability. Therefore, BODIPY fluorophores have been extensively used in the construction of molecular sensors. The emission of the parent BODIPY is usually in the green region and the Stokes shift is small (<20 nm) [4]. It should be stressed that a small Stokes shift is detrimental to the sensitivity of fluorescent molecular sensing systems. Interestingly, all the metal sensors based on BODIPY fluorophores show either short emission wavelength or small stokes shift. On the other hand, Ferrocene (Fc) is a very strong redox sensor showing excellent electrochemical sensitivity [5]. Fe (II) / Fe (III) redox couple is a perfect reversible electrochemical sensor. Cation coordination to an Fc host is expected to result in an anodic shift of the redox potential, making the Fc group more difficult to oxidize [6].

In Scheme 1, a representative structure for new designed BODIPY-Ferrosen based three channel sensors is shown, where Fc ring is linked to two BODIPY fluorophores via two linkers (bridges) and a Ca ion is trapped between these linkers.

Introduction of Ca(II) ion to designed sensor leads some important changes in the geometry. The two fluorine atoms are tilted toward the Ca ion. Geometric changes and restrictions play a key role in the electronic structure of the Fc [7].

In this work, it was aimed to design and computationally characterize Fc- BODIPY sensors of Ca(II) ion, for the use of possible future applications. It was also intended to investigate the trends in structural, electronic, redox, colorimetric and fluorescent properties of sensors against variations in the linker group. With these in mind, 4 models of BODIPY–Fc based sensors, having azine, azadiene, urea and thiazole groups as linkers, were constructed and their properties

Scheme 1
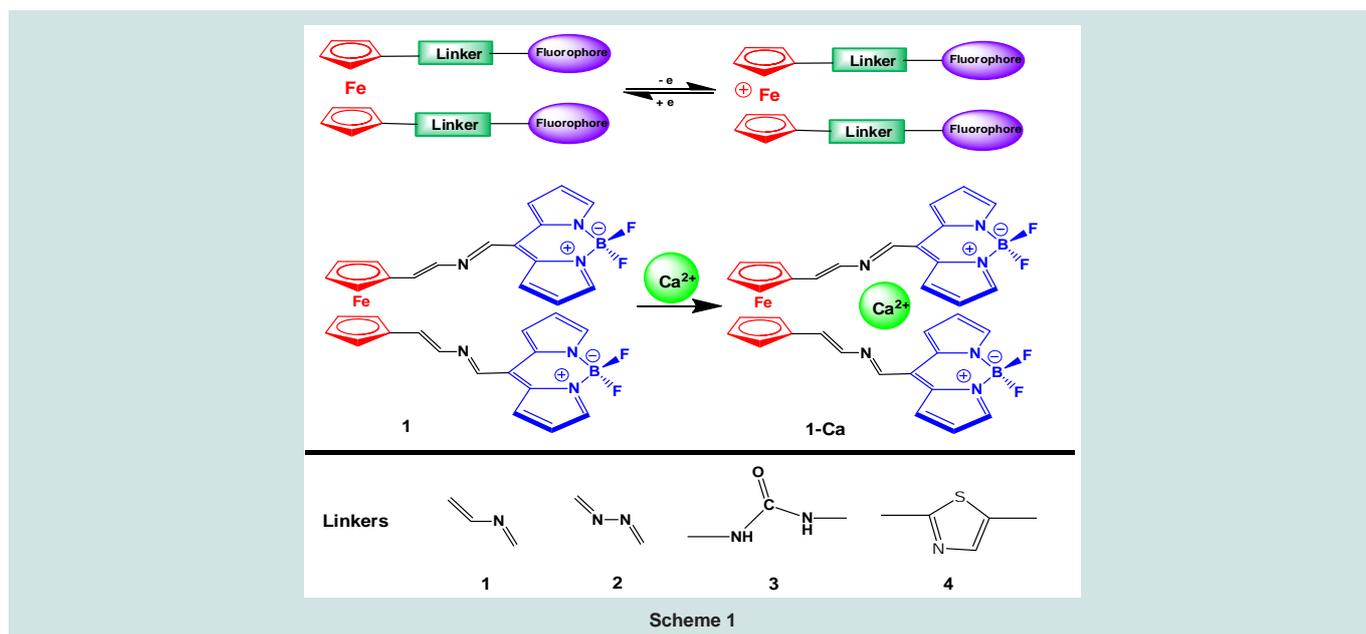
were determined computationally at B3LYP/LANL2DZ level of DFT. Also, molecular logic gates of these new designed sensors have been performed in acidic medium. Investigation of fluorescent molecular sensors from a theoretical perspective will improve our understanding of fluorescent sensors and will be helpful for designing new ones.

Calculation Methods

All calculations presented in this work were performed with the Gaussian 09 Revision C.0115 molecular modeling software using density functional theory (DFT) [8] methods, which can predict successful geometries, relative energies, and vibrational frequencies for transition metal complexes [9].

To determine the best DFT functional for the calculations of model structures, bond lengths and bond angles values for selected BODIPY structures from literature were computed at M06, B3LYP, B3PW91 and B3P86 levels of DFT and computational results were compared with corresponding experimental values. As a result, the overall performance of B3LYP functional was found to be better than the other three DFT functional, and all results presented in these work were found by using B3LYP functional (See supporting information for details). LANL2DZ basis set was applied. This basis set was found to be in good agreement with the experimental results in describing metal–carbon bonds for organometallic compounds in many cases [10].

All optimized geometries were also subjected to frequency analyses at the same level of optimization to verify the nature of the stationary points. Equilibrium geometries were characterized by the absence of imaginary frequencies in the reaction coordinate.

The time-dependent density functional theory (TDDFT) approach was used for the calculation of the vertical excitation energies in the UV-vis region.

In order to elucidate the interaction of designed structures with Ca (II) ions, Electrostatic Potential Surface maps are issued. A

7-digit TD-DFT method was used in emission calculation. The total energy of the structures (E), Gibbs free energy (W) and enthalpy (H) were calculated. Also, reduction potential of Fe (II) / Fe (III) redox couple, color changes and emission wavelengths were investigated. In addition, molecular logic gates were designed in acidic medium.

Results and Discussion

UV-visible absorption and emission spectra of the compounds

In Table 1, calculated spectroscopic parameters for designed sensors are seen. Binding the Ca ion to the sensor unit affected the UV-vis and fluorescence properties of sensors. Addition of Ca ion increases these values in an amount depending on the type of the bridging group as seen in Table 1. BODIPY unit has a major absorption peak (S0–S1 transition) near 500 nm. But incorporation of aryl susbstitutes and aza- substitution at the meso position push this peak into the red or blue end of the visible spectrum [11]. Further, using two fluorophores in a sensor, leads to longer absorption and emission wavelengths [12]. When results are compared, it is seen that the emission and absorption wavelengths are not overlapped and emission wavelengths are at longer values. In general, Maximum emission and absorption wavelengths of parent sensors are less than complexes. This sequence was also spotted in the acidic environment. In some of designed complexes emission and absorption wavelengths are shifted to NR-IR spectral region. These results, are defined as NIR dyes (red emitting fluorescent dyes), appear on the spectral properties of the compounds [13]. Spectrums can be found in Supporting Information in Figure S1.

Among designed BODIPY–Fc based sensors the highest absorption red shift, caused by insertion of Ca ion into the structure, belongs to **3** which is 286 nm and the lowest value is that of **4** which exhibits a change of only 7 nm. Considering the geometry of **4**, it is observed that Ca(II) ion is completely shifted toward the F atoms of BODIPY. Absorption wavelength in **2** increases by 228 nm and in **1**

Table 1: Spectroscopic data of designed Fc-BODIPY based sensors in water and acidic solutions.

Probe	Water phase				Acidic phase			
	λ abs.	λem.	Δλ	color	λ abs.	λem.	Δλ	color
1	667.56	725.15	57.59	-	639.67	682.06	42.30	Red
1-Ca	687.02	677.42	9.6	Red	597.02	618.94	21.92	Orange
2	564.2	607.82	43.62	Orange	699.03	716.18	17.15	-
2-Ca	792.31	985.01	192.70	-	686.42	843.27	156.85	-
3	587.36	854.97	267.61	-	597.65	989.13	391.48	-
3-Ca	873.21	939.02	65.81	-	816.06	894.91	78.85	-
4	577.12	695.31	118.19	Red	514.43	619.46	105.03	Orange
4-Ca	570.64	576.61	5.97	yellow	501.79	514.23	12.44	green

$\lambda_{abs.}$ & $\lambda_{em.}$: Maximum wave lengths of absorption and emission spectra,
Δλ: Difference between absorption λ_{max} and emission λ_{max}

Table 2: Thermodynamic values of complexation reactions of designed BODIPY-Fc based sensors with Ca(II) ion, (kcal/mol).

Structure	E^0	H^0	G^0	S^0
Ca(II)	-22865.96442	-22865.37206	-22876.39865	0.036983
1	1387917.967	-1387917.375	-1387989.522	0.241982
2	-1408031.071	-1408030.479	-1408102.721	0.242300
3	-1454716.065	-1454715.472	-1454787.755	0.242438
4	-1399093.136	-1399092.544	-1399163.271	0.237219
1-Ca	-1410781.235	-1410780.643	-1410854.392	0.247355
2-Ca	-1430905.653	-1430905.613	-1430979.621	0.248224
3-Ca	-1477582.109	-1477581.516	-1477651.699	0.235394
4-Ca	-1421991.810	-1421991.202	-1422065.267	0.248415
Reaction	ΔE_R	ΔH_R	ΔG_R	ΔS_R
1 → 1-Ca	2.69	2.10	11.52	-0.032
2 → 2-Ca	-8.62	-9.21	-0.51	-0.029
3 → 3-Ca	-0.08	-0.67	12.45	-0.005
4 → 4-Ca	-32.71	-23.28	-25.60	0.008

ΔE°: Total reaction energy, **ΔG°**: Free Gibbs energy of reaction, **ΔH°**: reaction Enthalpy
T= 298.15 K

by 20 nm. **1** and **3-Ca** have the longest wavelengths where bridging with thiyazole, **4**, decreased that to the lowest.

In **1** and **4** emission chemical shifts are found to be shifted towards lower magnetic fields with respect to the highest field signal of parent sensor. This effect is the most obvious in thiazole bridged structure which is about 119 nm. **2** has a red chemical shift value of 378 nm, where **3** has 85. **3** and **2-Ca** have the longest emission wavelengths, on the other hand, **2** and **4-Ca** own the lowest. Overall result of complexation is an increase in the λ_{max} value, while solvent effect causes a blue shift in bands.

Stabilities and fronteir molecular orbitals

In order to investigate thermodynamic properties of complexation reactions, the statistical thermodynamic calculations were carried out at 1 atm. and 298.15 K. The thermodynamic parameters such as binding energy (E°), Gibbs free energy (G°), enthalpy (H°) and entropy (S°) of each designed sensor and their complexes were calculated, to investigate the stability of formed complexes. The thermodynamic functions are given in Table 2. The stabilization energies are calculated with respect to the sum of electronic energies of the structures according to the designed below reactions as Eq. (1),

$$\Delta Estb = E°_{Ca-sensor} - E°_{Ca(II)} - E°_{sensor} \qquad (1)$$

The enthalpy values for the Complexation reaction of **4** is more endothermic than **3** and **2,** rendering **4** as a better Ca(II) ion acceptors. The ΔH values for the formation of **2-Ca** is less exothermic. Conversely **1** has an endothermic complexation reaction with Ca(II) ion.

The value for ΔS is also positive for **4**. The contact of the positive metal ion with the ligand donor atoms results in an effective charge neutralization and a positive entropy of association [14]. ΔS value is negative for formation of **1-Ca**, **2-Ca** and **3-Ca**. This is perhaps due to an increased metal-ligand bond distance in the XY plane of the metal ion.

Gibbs free energy reflects the trend of the spontaneous reaction.

Table 3: Frontier orbitals and reduction potential of designed structures in water phase.

Structure	Geometry	HOMO	E_H (eV)	LUMO	E_L (eV)	ΔE	Reduction Potential, E0 (V)
1			-6.00		-3.65	2.35	1.23
1-Ca			-6.09		-4.20	1.89	1.27
2			-6.30		-3.78	2.52	1.24
2-Ca			-6.28		-4.04	2.24	1.29
3			-5.85		-3.24	2.61	1.23
3-Ca			-5.88		-3.86	2.02	1.27
4			-6.26		-3.65	2.61	1.24
4-Ca			-6.23		-3.80	2.43	1.31
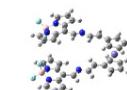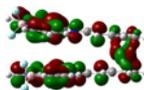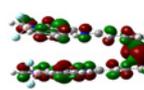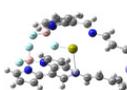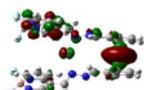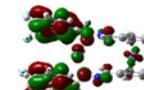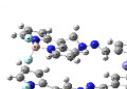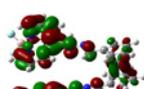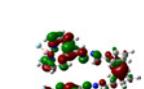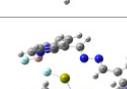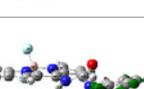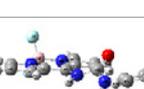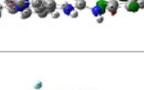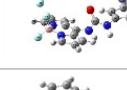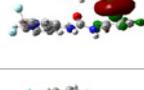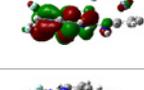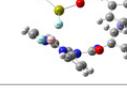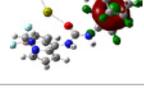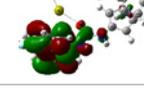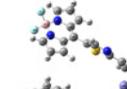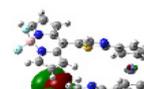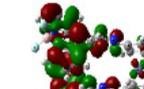
E_H: HOMO orbital energy, E_L: LUMO orbital energy
ΔE: Energy difference between HOMO and LUMO

Formation of **1-Ca** and **3-Ca** complexes resulted from slightly endergonic processes (ΔG° = 11.52 and 12.45) under the working level of theory. The result of the calculated Gibbs free energy change has greatly improved from +13.52 to -25.60. Binding of Ca(II) to **2** and **4** is slightly exergonic (ΔG° = -0.51 and -25.60). So, complexation of **4** and **3** has been found to be most and least stable, respectively and formation of **4-Ca** is preferred.

Negative and positive binding energies indicate stability and metastability of formed complexes. Binding energy of **4** is the lowest. It indicates that among these four designed sensors, **4** makes the most stable complexes. According to these thermodynamic results, tendency of our designed sensors to make an stable complex with Ca(II) ion is in this range **4>2>3>1**. This is in agreement with the results of energy gaps of Frontier orbitals.

When HOMO-LUMO molecular orbitals of designed sensors are analyzed (Table 3), we see that frontier orbitals are localized on whole molecule in **1** and **2**, while they are shifted on Fc and BODIPY moieties in **1-Ca** and **2-Ca**. MO orbitals of both **3** and **3-Ca** is on Fc and BODIPY units in respect. Sensor number **4** has its frontier orbital on BODIPY but HOMO is shifted toward Fc in **4-Ca**. Orbital shift is an indication of orbital motion of electrons.

The HOMO–LUMO gap is an important parameter to characterize

the electronic structure of molecules. According to the difference between the frontier orbitals energies, when the gap energy is higher, the system behaves like a stable molecule. Also the HOMO-LUMO gap is known to be the index of both kinetic stability (reactivity) and electrical conductivity. As it is known, the energy gap is lowered by the presence of conjugated π-systems in organic molecules. Therefore, the lower gap energies for Ca-complexes are attributed to the conjugated π-systems on the linkers. The smaller energy gap corresponds to the higher reactivity so that designed sensors can consider as the most reactive linkers. This decrement indicates stabilizing effect of Ca-complexes. It is seen that energy gap between HOMO and LUMO orbitals are reduced by adding metal ion into the structure. This decrement indicates stabilizing effect of Ca(II) on structures. For the HOMO-LUMO energy difference of the designed sensors, gap size increases from **1** to **4**. This order remains the same when Ca(II) ion enters to the structure. The biggest MOs energy gap belongs to **4-Ca**. The biggest difference in HOMO-LUMO energy belongs to sensor **3** and **4**. The lower the LUMO energy amount, the bigger is electron affinity [15]. Sensors behave differently because the fluorophore is perturbed by the expansion of the π-conjugation framework. Existing π-interaction on different linkers is an important factor of interaction of analyte molecule with the chromophore.

Electrochemical properties

One of the most important characteristics of Fc is that, electron affinity can be controlled by chemical or electrochemical redox reactions. Standard electrode potential of protonated structures

Table 4: Accuracy table of designed sensors.

Sensor	Input		Output	Molecular logic gate
	H⁺	Ca⁺²		
1	0	0	1 (725)	"NOR"
	1	0	0 (682)	
	0	1	0 (677)	
	1	1	0 (618)	
2	0	0	0(607)	"OR"
	1	0	1 (716)	
	0	1	1(985)	
	1	1	1 (843)	
3	0	0	0 (854)	"OR"
	1	0	1 (989)	
	0	1	1 (939)	
	1	1	1 (894)	
4	0	0	1 (695)	"NOR"
	1	0	0 (619)	
	0	1	0 (576)	
	1	1	0 (514)	
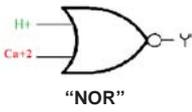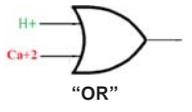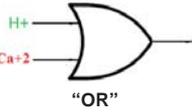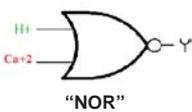
Output: Emission wavelengths in the presence of each ion
Molecular logic gate: Type of logic gate which designed sensor corresponds to

shown in Scheme 1 and their complexes, were calculated (Table 3). Protonation was performed through linker groups in designed sensors. Thus the redox reaction solution was found by using a thermochemical cycle.

4 has the highest redox potential. Increase of the oxidation potential upon substitution of the Cyclopentadiene ring, (CP), can be explained by the withdrawal of electron density from Fc moiety by substituents. If the Ferrocenium moiety is stabilized by some group, then the oxidation potential will be lower. Change in E^0 means changing in the electronic environmental of the molecule. The cation coordination to an Fc host sensor is expected to result in an anodic shift of the redox potential, making the Fc group more difficult to oxidize [16]. Binding a cation to the receiver unit causes a positive shift of the redox potential (Fc/Fc+) and the cause is electrostatic interactions The cation coordination to an Fc host sensor, is expected to result in an anodic shift of the redox potential, making the Fc group more difficult to oxidize [17]. Bigger anodic shift in redox potential means, higher charge density carrying potential, by guest or molecule, or by other words it can shift electron density toward itself [18]. According to electrochemical potential, complexation ability of the bridges can be controlled. Reduction potential of Fc is known to be 0.4(V) [19]. According to our results, reduction potential amount is increased by adding BODIPY linkers and Ca(II) ion to the structures. Changes in the reduction potential values are an indication of cation connection to the bridge and also show bonds strength. Between reduction potential of designed sensors, which are shown in Table 3, parent sensors have lower reduction potential values than complexes. The biggest reduction potential belongs to **4-Ca** and the sensor **1** and **3** own the lowest.

Molecular Logic Gates

The use of Molecular Logic Gates in biochemical researches is very new and has started to improve. In Chemical logic systems, binding of a guest molecule to the host compound forms a logic input and results changes in absorption and/or fluorescence spectra, including physical changes (output) [20]. Logic of computing is based on bits that can be written and read as 0 or 1. This is achievable in molecules as in many ways, but the most common are based on switching the optical properties of the molecule. Fluorescent chemosensing is useful in biomedical research and it has been very recently developed into chemical logics. In the chemical logic system, the binding of a guest molecule to a host compound corresponds to the logic input and the resulting physical property change such as absorption and/or fluorescence spectra corresponds to the logic output.

In this research, molecular logic gates are formed for normally protonated and metal complexes of designed Fc-BODIPY based sensors which have shift in the emission spectrum. Accuracy tables of the sensors are given based on the calculated emission and absorption λ_{max} in water phase and acidic medium. Calculated absorption and emission wavelengths, in water phase and in acidic medium, are shown in Table 1 also.

Hydrogen and Calcium ions are considered as two inputs here. Emission wavelengths in the presence of Ca(II) ion in the acidic phase create output signals. The logic state of a terminal can, and generally does, change often, as the system processes data. Judging the accuracy

table of statements given in Table 4, sensors **1** and **4** corresponds to NOR sign of logic gates. The NOR gate is a combination OR gate followed by an inverter. Its output is "true" if both inputs are "false". Otherwise, the output is "false" [21]. Fluorescence from 725 and 695 are switched 'OFF' by Ca^{2+}. Similar action of H^+ can also be seen. Here, the cations do not induce an enhanced emission from sensors.

In sensors **2** and **3**, when two cations were added separately or all together as inputs, emission is significantly enhanced above the threshold. Thus, all three metal ion inputs are required simultaneously or separately for the emission increase; this behavior is in accordance with an OR logic gate. The **OR** gate gets its name from the fact that it behaves after the fashion of the logical inclusive "or". The output is "true" if either or both of the inputs are "true". If both inputs are "false," then the output is "false". The **OR** gate requires a set of nonselective receptors gives a positive optical response upon cation binding. The less selective the receptor, the operationally better **OR** action [22]. Both cations caused similar conformational changes in the receptor unit. The reason why the gate response is such can be explained in this way: Normally, with what we have discovered about BODIPY – Fc based sensors, one should expect low fluorescence output at long wavelength whenever fluoride is present on BODIPY moiety. But, when together with Ca(II) situation is different, because fluoride has a higher affinity for the chelated Ca(II)center.

Conclusion

According to the results of this study, for new designed BODIPY-Fc based Ca(II) sensors, **4** and **2** makes the most stable complexes with Ca(II) ion and it is proved, by thermodynamic calculations, that the decreasing order of desired complexation reaction is: **4→4-Ca>2→2-Ca>3→3-Ca>1→1-Ca**.

When spectroscopic properties are considered, we see parent sensors have bigger absorption wavelengths than complexes, increasing the red shift effect from 7 nm in **4** up to about 386 nm in **3** (**3>2>4>1**). Computed emission λ_{max} values of **1-Ca** and **4-Ca** were observed shorter than their parent sensors. Among the other complexes, those having higher red shift, have also longer emission λ_{max} values. In general, complex formation causes a decrease in the energies of both the HOMO and LUMO with respect to the linker group types, which results in the end with a decrease in HOMO-LUMO gaps. HOMO-LUMO energy gap decreases with introducing Ca ion into the sensors structures in this order **4-Ca>2-Ca>3-Ca>1-Ca**. Another parameter indicating the stability of 4-Ca is redox potential, in other words, increasing amount of redox potential from 1 to 4 proves the difficulty of reduction through an electrochemical reaction, **4-Ca>2-Ca>3-Ca>1-Ca**. Electrochemical investigation of designed sensors reveals an anodic shift of redox potential, by adding Ca(II) ion into the sensors. The biggest anodic shift belongs to **4-Ca** (**4>2>3 = 1**). When molecular logic gates are proposed for normally protonated and metal complexes, it was found that each type of designed sensors are corresponded to **NOR** and **OR** gates.

As a result, we believe that our complementary theoretical investigations on the Fc- BODIPY molecular probes will be useful to be experimentaly designed, with predetermined photophysical properties. As an example a new type of donor– acceptor molecule DiFc-B combined Fc and BODIPY unit has been synthesized by Daoben Zhu and coworkers, and the photophysical property, and

electrochemical property have studied [23]. A notable absorption change had been observed when metal ion was added to the compound. The energy gap between the HOMO and LUMO, spectral data and electrochemical results had a good consistence with our theoretical studies.

Consequently, the absorption and emission wavelengths and the experimental results are in line with the known fact that the DFT calculations usually underestimate the excitation energy for the transitions. Despite of some little discrepancy between the calculation and the experimental results, the DFT/TDDFT calculations clearly predicted the red shift of the absorption and fluorescence of probes upon interaction with Ca(II), the colorimetric and ratiometric fluorescence changes.

References

1. Rochford J, Rooney AR, Pryce MT (2007) Redox control of meso-Zinc(II) ferrocenylporphyrin based fluorescence switches. Inorg Chem 46: 7247-7249.

2. Turfan B, Akkaya E (2002) Modulation of boradiazaindacene emission by cation- mediated oxidative PET. Org Lett 4: 2857-2859.

3. Caballero A, Espinosa A, Tárraga A, Molina P (2008) Ferrocene-based small molecules for dual-channel sensing of heavy– and transition- metal cations. J Org Chem 73: 5489-5497.

4. Shao J, Sun H, Guo H, Ji S, Zhao J, et al. (2012) A highly selective red-emitting FRET fluorescent molecular probe derived from BODIPY for the detection of cysteine and homocysteine: an experimental and theoretical study. Chem Sci 3: 1049-1061.

5. Boens N, Leen V, Dehaen W (2012) Fluorescent indicators based on BODIPY. Chem Soc Rev 41: 1130-1172.

6. Alfonso M, Tárraga A, Molina P (2011) Ferrocene- based heteroditopic receptors displaying high selectivity toward lead and mercury metal cations through different channels. J Org Chem 76: 939-947.

7. Yin X, Li Y, Li Y, Zhu Y, Tang X, et al. (2009) Electrochromism based on the charge transfer process in a ferrocene–BODIPY molecule. Elsevier 65: 8373-8377.

8. Kohn W, Sham LJ (1964) Self-Consistent equations including exchange and correlation effects in homogeneous electron gas. Phys Rev 140: A1133-A1138.

9. Bühl M, Reimann C, Pantazis DA, Bredow T, Neese F (2008) Geometries of third-row transition-metal complexes from density-functional Theory. J Chem Theory Comput 4: 1449-1459.

10. Zhang X, Schwarz H (2010) Bonding in cationic MCH2+ (M=K–La, Hf–Rn): A theoretical study on periodic trends. Chemistry 16: 5882-5888.

11. Bozdemir OA, Guliyev R, Buyukcakir O, Selcuk S, Kolemen S (2010) Selective manipulation of ICT and PET processes in styryl-Bodipy derivatives: Applications in molecular logic and fluorescence sensing of metal Ions. J Am Chem Soc 132: 8029-8036.

12. Cakmak Y, Kolemen S, Duman S, Dede Y, Dolen Y (2011) Designing excited states: Theory- guided access to efficient photosensitizers for photo dynamic action. Angewandte Chemie 50: 11937-11941.

13. Sunahara H, Urano Y, Kojima H, Nagano T (2007) Design and synthesis of a library of BODIPY-based environmental polarity sensors utilizing photo induced electron-transfer-controlled fluorescence ON/OFF switching. J Am Chem Soc 129: 5597-5604.

14. Letter JE, Bauman JE (1970) A thermodynamic study of the complexation reactions for a series of amino acids related to serine with Copper (11) and Nickel (11). J Am Chem Soc 92: 437-442.

15. Yoshii R, Yamane H, Nagai A, Tanaka K, Taka H (2014) π-Conjugated

polymers composed of BODIPY or Aza-BODIPY derivatives exhibiting high electron mobility and low threshold voltage in electron-only devices. Macromolecules 47: 2316-2323.

16. Honglan Qi, Teesdale JJ, Pupillo RC, Rosenthal J, Bard Aj (2013) Synthesis, electrochemistry, and electrogenerated chemiluminescence of two BODIPY-appended bipyridine homologues. J Am Chem Soc 135: 13558-13566.

17. Roggers EI, Silvester DS, Poole DL, Aldous L, Compton RG (2008) Voltammetric characterization of the Ferrocene/Ferrocenium and Cobatocenium/Cobaltocene redox couple in RTILs. J Phy Chem 112: 2729-2735.

18. Nepomnyashchii AB, Bard AJ (2011) Electrochemistry and electrogenerated Chemiluminescence of BODIPY Dyes. Acc Chem Res 45: 1844-1853.

19. Guliyev R, Ozturk S, Kostereli Z, Akkaya EU (2011) From virtual to physical: Integration of chemical logic gates. Angewandte Chemie 50: 9826-9831.

20. Baytekin T, Akkaya E (2000) A molecular NAND gate based on Watson−Crick base pairing. Org Lett 2: 1725-1727.

21. Coşkun A (2003) Novel supramolecular ion sensing systems and their application in molecular logic gates. A thesis submitted to the graduate school of natural and applied sciences of the middle east Technical University.

22. Andreasson J, Pischel U (2015) Molecules with a sense of logic: a progress report. Chem Soc Rev 44: 1053-1069.

23. Yin X, Li Y, Li Y, Zhu Y, Tang X (2009) Electrochromism based on the charge transfer process in a Ferrocene- BODIPY molecule. Elsevier 65: 8373-8377.

Acknowledgements